Physicochem. Probl. Miner. Process., 55(4), 2019, 1002-1013

http://www.journalssystem.com/ppmp

Physicochemical Problems of Mineral Processing

ISSN 1643-1049

Received February 02, 2019; reviewed; accepted March 19, 2019

Determination of mineral surface energy using impact of rough topography

Muhammed Fatih Can, Caner Çiftçi

Afyon Kocatepe University, Engineering Faculty, Mining Engineering Department, Afyonkarahisar, Turkey

Corresponding author: mfcan@aku.edu.tr (Muhammed Fatih Can)

Abstract: While some of the studies on the functionalization of surfaces are still in theoretical phase, it is not possible to apply them on natural surfaces which already contain some irregularities. However, progress can be made with a mineral having significant purity, crystal homogeneity, and controllable surface workability for surface treatment operations. Therefore, in this study the effects of roughness on the surface energies of natural stones were investigated by selecting a sample with a distinctive color and metamorphic origin from Mugla, Turkey. First, sample surfaces were prepared using a polishing line with five different abrasives. Three-dimensional surface scans were then performed with ZYGONewView7100 optical-profilometer and ParkSystemAFM to identify the 3D roughness of the surfaces on two different scales (micro and nano) with SPIP-software. The micro average heights (S_a) of the produced surfaces ranged between 0.423-1.127 μm, nano-scale 0.0806-0.173 μm, while the surface roughness ratio (S_{dr}) between 33.7%-40.1%, and nano-scale 5.19%-18.5%. The contact angles of the samples were measured in the presence of pure water, formamide, and diiodomethane using AttensionTheta-tensiometer. Changes in surface energy were followed by Van Oss, Good-Chaudrey approach. Young, Wenzel, Cassie-Baxter contact angle theories were tested within these calculations. It was revealed that the inconsistency in solid phase energy could not be determined at this stage, but it could be regulated by modifying the Cassie-Baxter approach. Furthermore, the percentage of air packs likely to be below the water droplet not foreseen by the previous studies was calculated as 26% up to 35% air gap on the solid/water interface.

Keywords: micro-nano roughness, natural stones, surface energy, air gap

1. Introduction

With a generalized perspective, among the studies performed using the roughness of a surface, the reviews on the identification and imitation of the unusual features of natural surfaces (lotus leaf, etc.) are quite common (Hill, & Bico, 2006; Ma et al, 2009; Greßler et al., 2010; Su, 2010). Moreover, studies on the production of these functionalized surfaces have become more widespread in the last two decades. Among these, a striking point is that they consist the artificial creation of imitated natural surfaces. However, the intrinsic roughness of natural surfaces has been investigated thoroughly on the flotation enrichment process that depends on the wettability and hydrophobicity difference of the minerals. For a more in-depth study on flotation behaviors of grains whose final roughness effected by the grinding media; flotation recovery, bubble retention, and contact angle changes in the presence of additional surfactant were followed (Yekeler et al., 2004; Ahmed, 2010; Karakas & Hassas, 2016; Hassas et al., 2016). Furthermore, the approaches used to express the change of surface energies in applications are constantly evolving throughout the historical process due to the increasing complexity of the problems and the developing techniques.

The first studies on the determination of surface energy is dated back to the 1800s. Prof. Thomas Young published his work "An essay on cohesion of fluids"in the journal of Philosophical Transactions of the Royal Society of London (Young, 1805). Young described the state of the liquid

DOI: 10.5277/ppmp19022

drop on a smooth and chemically homogeneous solid surface with solid-liquid, liquid-air, and solid-air phases. He expressed the force balance between these phases with Young's contact angle. His equation is too general although being well celebrated, thus being not able to provide any quantitative descriptions about the energetical states of the interphase boundaries.

Young ’s approach was further developed in 20th century, by series of pioneering works (Fowkes, 1963; Zisman, 1964; Owens & Wendt, 1969; Neumann et al., 1974; Van Oss et al., 1988). The common point of these works was the definition of solid surface energy using the balances formed by applying more than one pure liquid on the smooth solid. Simply, this new theoretical development (see the above literature) is meant to quantify the energy of natural solid surfaces, assuming that they are flat and energetically homogeneous. Much of the research has been concentrated on synthetic surfaces (Dorrer & Rühe, 2009; Liu et al., 2010; Itherm, 2015). The surfaces are naturally rough, and may contain more than one structural component. Neuman et al. stated that natural surfaces might produce different results in the measurement of the energy of solid surfaces (Neumann et al., 1974). Wu and Van Oss in their study showed that the contact angles measured on the surface of optically clear calcite crystal and ground calcite were different from that measured with calcite powder saturated with moisture (Wu & Van Oss, 1996). In this context, it is thought that another factor may be useful in the determination of solid surface energy.

Wenzel (Wenzel, 1936) and Cassie-Baxter (Cassie & Baxter, 1944) studied the effects of the topography of the solid surface on its surface energy. Wenzel introduced the roughness factor as the ratio of the actual asperities to the geometric area below a drop situated on the solid and revealed the correlation between the experimentally measured contact angle and the Young contact angle on rough surfaces. The increase of the surface roughness of hydrophobic surfaces usually elevates their level of hydrophobicity significantly. The opposite is valid for hydrophilic surfaces. Unlike the other authors (Young, Wenzel, etc.) Cassie defined different components of the surface and the impact of each one of them on the overall contact angle of droplet situated on a solid surface. (Milne & Amirfazli, 2012; Zhao, et al., 2013; Hejazi, 2014). Following Cassie's work, Cassie and Baxter stated that there could be a two-component structure consisting of solid-liquid (first component) and liquid-air (second component) phases at the solid surface (Cassie et al., 1944; Choi et al., 2009; Murakami, et al., 2014). This second component (the liquid-air phase) exists in the form of air packs underneath the liquid drop (Jung & Bhushan, 2008). Moreover, it has been shown that nano air packages can form on the solid structures (Gao & Yan, 2009; Starov, 2010; Fritzsche & Peuker, 2014; Ditscherlein et al., 2016; Wang et al., 2017). Their formation is based on a completely different balance on the rough surfaces, like the formation mechanism of the micro-air packs on the rough surface (Hampton & Nguyen, 2010; Wang et al., 2015).

In the studies on ore preparation and enrichment, along with a number of parameters of the particles (e.g. total surface area , the shape of the particles, zeta potential, *etc.*), their hydrophobicity has been proven to be important, because it is closely related to their surface energy (Hicyilmaz et. al., 2005; Rahimi et.al., 2012). From this point, in the light of the above surface energy detection studies, we took another step here, and examined the reaction of a mineral surface to liquids with different surface energies in addition to a detailed multi-dimensional surface investigation. As a contribution to research on natural surfaces, the effect of the production method conditions on the functionalization of natural stone surfaces were produced, as surface coating materials in architectural structures, was observed. As a primary step, the knowledge necessary to understand such a natural mineral surface should be assessed following the entire historical development of the surface chemistry. Only in such a case one use the physical parameters to manipulate the contact angle of the surfaces.

2. Material Methods

The Mugla white marble sample, used in this study, was determined to be composed of pure calcite crystal in the analysis by Rigaku ZSX brand XRF device (Table 1). The surface of the marble was examined in three directions by a polarizing microscope, and as a result, calcite crystals were found to have a perfectly fine granoblastic texture (Fig. 1).

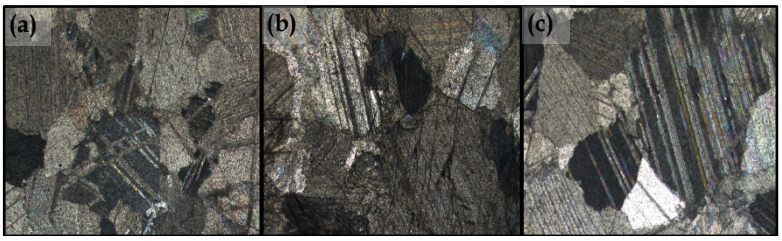

Fig. 1. Thin section images of Mugla white marble, (a) x axis, (b) y axis, and (c) z axis.

Table 1. Chemical composition of Mugla white marble by wt.%.

Chemical Composition									
SiO_2	Al_2O_3	Fe_2O_3	MgO	CaO	Na_2O	K_2O	Ti_2O	MnO	LOI*
0.12	<0.01	0.04	0.36	56.17	0.03	<0.01	0.01	<0.01	43.3

* Loss of Ignition (LOI)

The samples obtained from the Muğla region were processed as a plate in a factory. To differentiate the surface parameters in this study, the samples were passed through the Toyamer brand polishing line consisting of four abrasive and two caliber heads. The surfaces were polished with abrasive heads of 116 - 68 - 36 - 23.6 - 16 µm in a manner described in Table 2. Then, the samples were cut to 10 cm x 10 cm, and cleaned with pure water, and dried in an oven at 60 °C. Attension Theta brand contact angle device was used to measure contact angle with pure water, diiodomethane, and formamide liquids at 20 °C. Park System brand AFM, Zygo Newview 7100 optical profilometer and Leo brand SEM were used to determine the surface topography of the samples. The AFM scan size was 10 x 10 µm, and the profilometer scan size is 140 x 180 µm. Images were examined in two stages. In the first stage, the micro-size roughness parameters obtained from the profilometry measurements, where nano-size parameters obtained from AFM raw images were determined by SPIP program, and later the surface energy evaluations were performed with calculated data. According to the method applied by LaMarche et al. the roughness of the nanostructures on the surface was separated, and the roughness parameters were re-calculated (LaMarche, 2017). Then, SPIP three-dimensional roughness parameters S_a, S_{dr}, and 2-dimensional roughness parameter R_a values were determined (ISO 4287, ISO 25178). Young, Cassie-Baxter and Wenzel approaches were tested.

Table 2. The surface treatment process applied to the polishing line.

Sample code	Polishing Process
1M	116
2M	116+68
3M	116+68+36
4M	116+68+36+23.6
5M	116+68+36+23.6+16

2.1. Van Oss – Good - Chaudhury Acid-Base Theory (C. J. Van Oss et al., 1988)

The acid-base approach of van Oss et al. (Van Oss et al., 1988) was used to determine the density of the surface energy (surface tension) γ_S of the solid surface. It is composed of two components -polar (Lewis acid-base electron donor-electron acceptor) and nonpolar (Lifshitz-van der Waals) γ_S^{LW} ones. The Lewis acid-base component of the surface tension consists of Lewis acid (electron acceptor) γ_S^+ and Lewis base (electron donor) γ_S^- substituents. The surface tension of the liquids is described through the same components - γ_L^{LW} γ_L^+, and γ_L^-. The surface tension components of the solid surface γ_S^{LW} γ_S^+, and γ_S^- can be determined if the Young contact angles of small droplets of two polar, and one nonpolar, liquid with known values of γ_L^{LW} γ_L^+, and γ_L^- at the solid surface are measured (Fig. 2).

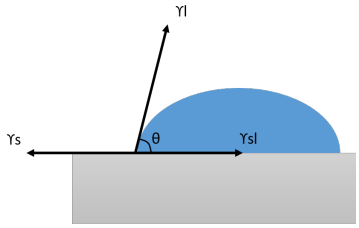

Fig. 2. Three-phase contact angle

Here, water and formamide were used as polar, and diiodomethane as nonpolar liquids. The following relation between the Young contact angle θ and the above-mentioned components of the solid and liquid surface tensions were used (Van Oss et al., 1988):

$$\left(1+\cos\theta_Y\right)\gamma_L = 2\left(\sqrt{\gamma_S^{LW}\gamma_L^{LW}} + \sqrt{\gamma_S^{+}\gamma_L^{-}} + \sqrt{\gamma_S^{-}\gamma_L^{+}}\right) \tag{1}$$

$$\gamma_S^{AB} = 2\sqrt{\gamma_S^{+}\gamma_S^{-}} \tag{2}$$

$$\gamma_S = \gamma_S^{AB} + \gamma_S^{LW} \tag{3}$$

where γ_S is the surface tension of the solid with its substituents Lewis acid-base γ_S^{AB} and Lifshitz-van der Waals substituents γ_S^{LW} (see Eq.3).

2.2. Young Approach

According to the Young approach, there is a relationship between the surface energy of a homogeneous solid layer and the contact angle measured with the liquid drop on it. In the current study, energy calculations were made using the acid-base interaction theory with the apparent contact angle data (θ_Y).

$$\gamma_S = \gamma_{SL} + \gamma_L \cos\theta_Y \tag{4}$$

where γ_S is the surface tension of the solid surface, γ_{SL} is the interfacial tension between the solid and liquid, while is the surface tension the liquid.

2.3. Wenzel Approach

Wenzel stated that, when a drop of liquid was placed on a solid surface, roughness of the surface affected the contact angle of the drop (Fig. 3) (Wenzel, 1936). The Wenzel approach expressed the relationship between a rough surface and a flat surface as a roughness factor (R_f) (Eq. 5). In this approach, the surface tension of the solid was calculated by using the van Oss acid-base theory. The calculation of the surface tension of the solid was performed by taking the roughness values of the measurements in nano (R_{fn}) and micro (R_{fm}) dimensions into account.

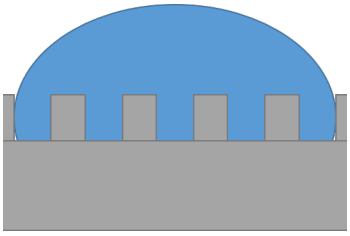

Fig. 3. Liquid wetting solid according to Wenzel

$$\cos\theta_W = R_f \cos\theta_Y \tag{5}$$

The Young contact angle θ_Y is expressed utilizing the apparent contact angle θ_W rough surfaces by combining the roughness factor R_f. The surface macro-roughness factor and the nano-roughness factor is represented by R_{fm} and R_{fn} are further discussed in the "Results" section.

2.4. Cassie Approach

Cassie expressed the relationship between the free surface energy of the system and the contact angle of the different components on the surface.

$$\cos\theta c = \Sigma f_i * \cos\theta_i \tag{6}$$

The spatial ratio f_i of the component on the surface, θ_i the contact angle value measured in the field. The two components (Fig. 4) are expressed as follows for the system.

$$\cos\theta_C = \cos\theta_A * f_1 + \cos\theta_B * f_2 \tag{7}$$

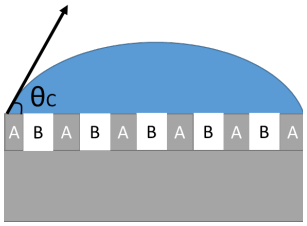

Fig. 4. Surface components according to Cassie approach

2.5. Cassie-Baxter Approach

According to the Cassie-Baxter approach, there may be air gaps between the topographic projections of a rough solid surface (Fig. 5). Thus Cassie-Baxter equation reads:

$$\cos\theta_{CB} = R_f \cos\theta_Y - f_{LV}\left(R_f \cos\theta_Y + 1\right) \tag{8}$$

In Eq. 7, f_{LV} = liquid-air interface ratio and f_{SL} = solid-liquid interface ratio. The total of the solid surface (f_{SL}) to which the liquid is contacted to solid ratio and the (f_{LV}) liquid suspended ratio is "1". " θ_Y " the Young contact angle, " θ_{CB}" rough surface contact angle and " R_f" refers to roughness ratio as mentioned in Wenzel approach.

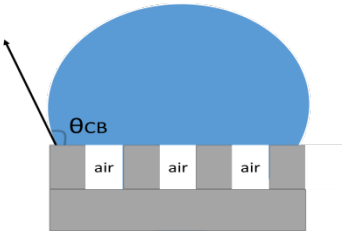

Fig. 5. Solid/Liquid interaction on a rough surface according to Cassie Baxter

3. Results and discussion

3.1. Surface topography characterization

The five surfaces produced as presented in Table 2 were subjected to thorough surface inspection to assess the micro and nanoscale roughness. The consistency of the optical profilometer and AFM methods used in the digitization of the surfaces was cross-checked by SEM imaging performed with

various magnification values (500, and 5000 X). In addition to the change of the valleys and peaks of scratches caused by microscale abrasives, the break/wear characteristics of the material with the trigonal crystal structure (Matziaris & Panayiotou, 2014) on the nanoscale was observed (Fig. 6.).

Fig. 6. Profilometer, AFM, and SEM images

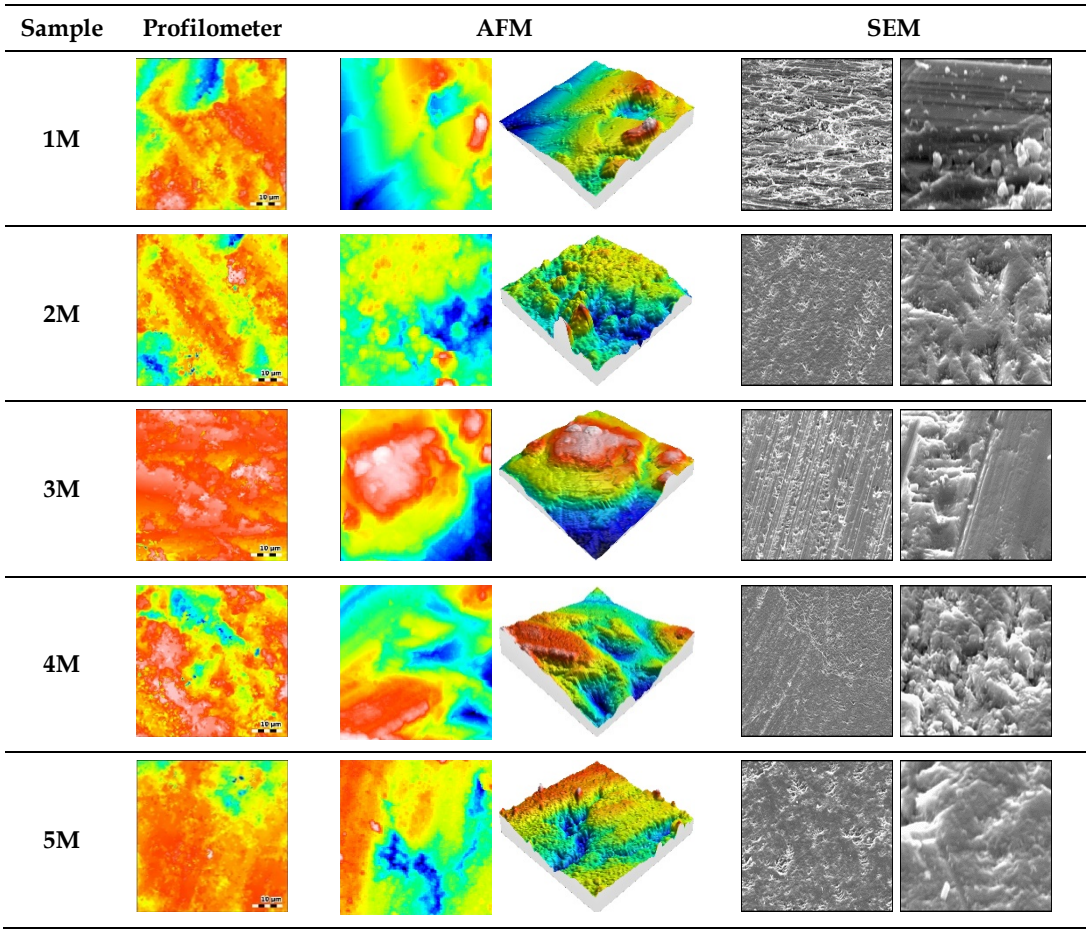

Images obtained from optical profilometry and AFM were processed in SPIP analysis program and R_a (2D arithmetical mean height), S_a (3D arithmetical mean height), S_{dr} (area increase compared to a flat surface/calculated area over the projected area) values were calculated for each sample according to the obtained data (Table 3). Notably, the S_{dr} value presented here are used in Wenzel, and Cassie Baxter approaches as the R_f value in Eqs. 5 and 7. Due to the reduced attrition of the abrasives as the mesh values increased, the micro- and nano-sized R_a values decreased as it progressed from 1 M to 5 M samples. A similar decrease was observed in the S_a values. The S_{dr} showed a decrease in micro-size but increased in nano-size. When the size of the abrasive grain decreases, it cannot break large parts from the crystal surface but create new surfaces in nano size.

Table 3 SPIP 3D roughness analysis

Sample	Roughness					
	R_a (nm)	R_a (nm)	S_a (nm)	S_a (nm)	S_{dr} (%)	S_{dr} (%)
	Nano	Micro	Nano	Micro	Nano	Micro
1M	44.3	240	173	1127	5.19	45.2
2M	33.25	188	125	676	14.7	39.7
3M	15.5	145	95.6	582	16	40.1
4M	14.2	109	70.1	511	18.5	45.5
5M	9.1	86.2	63.4	423	6.85	33.7

The studies using contact line profilometers (Tantussi & Lanzetta, 2007; Gürcan & Öztürk, 2014), which traditionally measure surface roughness in 2D, included coverage error. It was demonstrated in repeated measurements that the 3D roughness value of S_a was more inclusive than any other parameters. The average ratio of S_a values between the micro and nano scales, which are the basis of our study, was found to be 5.5 times increased, but there was no definite distinction in micro and nano dimensions. To avoid interferences between the different measurements performed on these surfaces, which are observed to contain a hierarchical pattern, LaMarche et al. (2017) methods are used on the natural hierarchical surfaces, and the optical profilometer data which is taken in large size is divided into micro and nano dimensions.

A range of scales has been found when searching for a hierarchical structure assessment in which the proportion of coarse and fine parts should be defined. He et al. (2014) on the hydrophobic silicon surface, the width of the microstructures in the hierarchical structures defined as 20 μm, the width of the nanostructure is 0.2 μm. Kim et al. (2013) in his work on aluminum and boehmite said that the grain size in hierarchical structures was 125 μm to 10 nm. In studies on natural hydrophobic hierarchical surfaces, the separation of micro and nano size is generally expressed as >1 μm micro dimension, 0.2 μm nano size (Webb et al., 2014; Wu et al., 2016). Although, there is no generalized distinction dimension in literature, it has been found that the smallest ratio between micro and nanoroughness is 5 (Hejazi et al., 2014).

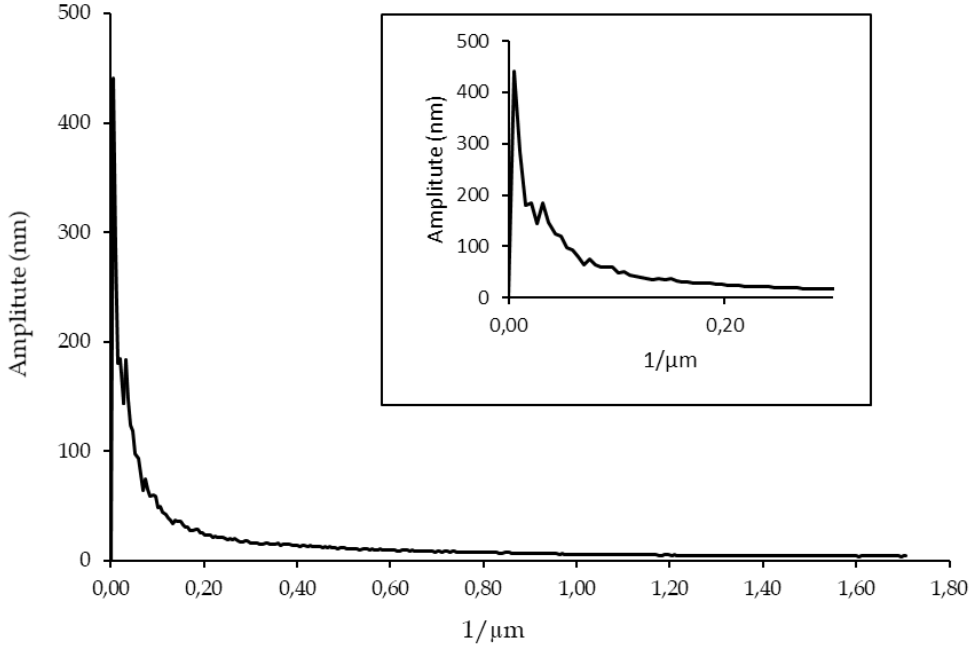

Fig. 7. Fourier transform of 1M sample as an example. a) Further focused to define the exact breakthrough point

As explained by LaMarche et al. (2017), the Fourier transform should be calculated with the elevation values taken from the 3D optical profilometer data and by examining the graphic the point at which the curve slope decreases and begins to convert horizontally should be determined. After the fast Fourier transform (FFT) of the roughness of each surface on the multiple scales completed with SPIP software, nano-roughness above the frequencies higher than 0.20 μm-1 was separated (Fig. 7). Roughness below 0.20 μm-1 is expressed as micro-roughness. The nano roughness removal carried out at this stage is shown as the micropattern and normalized nano pattern by separating the original profile as seen in Fig. 8.

The nano-roughness of the frequencies above 0.20 μm-1 showed compatibility with the R_a and S_a values obtained from AFM. The change in roughness values measured by AFM and profilometer, and FFT results showed similar character. From this point of view, FFT surface characterization gave meaningful value for roughness determination. In Table 4, which contains the analysis data re-prepared, reveals the R_a and S_a values approach each other on a micro scale. What is more critical in

this table is the proximity of the nano R_a and S_a values to the AFM values. After this point, there will not be an excessive evaluation of the hierarchical structure accounts because there will be no interference from each of the two scales.

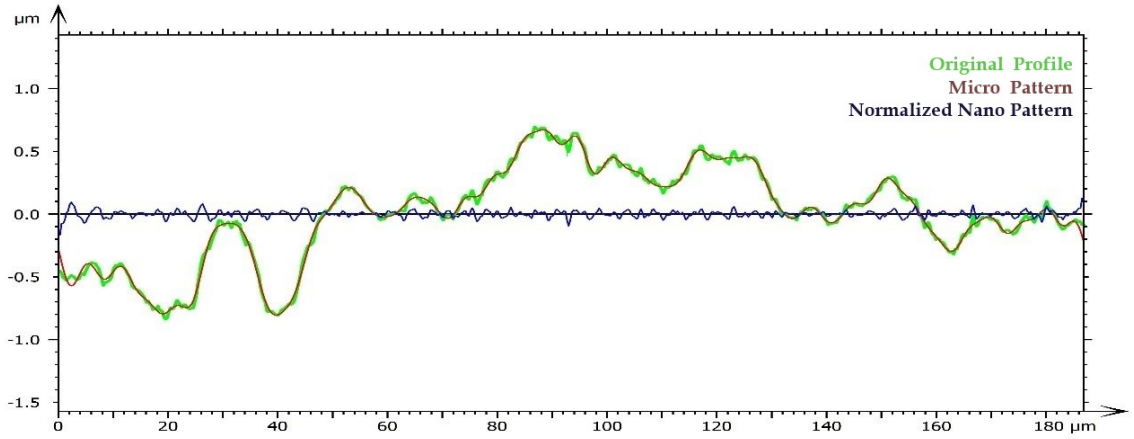

Fig. 8. The disintegration of a 2D topography profile into micro and nanopattern

Table 4. Re-calculated roughness analysis parameters

Sample	Profilometer		AFM	Profilometer		AFM
	R_a (nm) Nano	R_a (nm) Micro	R_a (nm)	S_a (nm) Nano	S_a (nm) Micro	S_a (nm)
1M	187	872	173	188	903	173
2M	167	860	125	167	856	153
3M	346	452	95.6	336	488	311
4M	216	1663	70.1	286	1698	304
5M	133	1100	63.4	133	1020	123

3.2. Surface energy evaluation

When the data were interpreted with the Young approach, it was not possible to obtain only one surface energy for the solid (Table 5). It was thought that the determination of different surface energies on the solid could be related to the surface topography, so the Wenzel approach (Eq.5) was tested, and the surface energy of the solid was determined by taking the roughness into account. Single surface energy could not be obtained with the Wenzel approach. Due to different surface energies, it can be assumed that there is another "B" component of the solid besides the different roughness. As known from literature that different components may affect the contact angle as indicated in the Cassie approach (Eq. 6). However, the calcite crystal, which is the subject matter, is almost pure (> 99.7% purity), and its impurities cannot cause a deviation of this magnitude.

Table 5. Measured contact angles and calculated solid surface energy

Sample	Contact Angle (°)			Young Solid Surface Tension (mN/m)	Wenzel Solid Surface Tension (mN/m)
	Water	Formamide	Diiodomethane		
1M	30.5	17.4	34.7	55.3	38.1
2M	36.9	23.4	30.0	53.8	35.9
3M	40.4	19.2	30.3	55.6	36.7
4M	44.9	32.2	40.2	49.9	33.7
5M	34.4	15.2	37.0	56.2	40.8

In this case, it is evident that heterogeneous wetting regimes are frequently defined on hydrophobic surfaces (Hejazi, 2014). However, with some detailed examination, some researchers

have identified the presence of nanobubbles on the surfaces of hydrophilic alumina (Ditscherlein, 2016), as is the surface of nanostructured PMMA (Wang, 2017) with macroscopic contact angle of 63.7. Under these conditions, proof of the existence of such air bubbles in the respective interfaces may be required, but the existence of bubbles is accepted as the reason for the existing divergence for experimental convenience. However, the "f_{LV}" component, which may influence the solid surface to this extent, maybe air packs as indicated in the Cassie-Baxter approach (Eq. 7). Here, the presence of air packs is taken as an assumption, and the Young contact angle measured by Wu et. al. (1996) on the calcite crystal (Pure Water: 6.2 °, Formamide 7.2 °, Diiodomethane: 38.5 °) was used to determine the possible amount of air gaps in the study.

Table 6. Predicted air gap ratios under liquid drop (f_{LV}) according to the Cassie-Baxter approach

Predicted air gap ratios at the solid/liquid interface					
			Pure Water		
Size	1M	2M	3M	4M	5M
Nano	0.093	0.159	0.182	0.216	0.166
Micro	0.238	0.247	0.264	0.277	0.216
Micro&Nano	0.264	0.306	0.326	0.346	0.295
			Formamide		
Nano	0.047	0.103	0.096	0.151	0.101
Micro	0.199	0.196	0.186	0.217	0.155
Micro&Nano	0.226	0.259	0.256	0.293	0.240
			Diiodomethane		
Nano	0.00	0.02	0.02	0.09	0.071
Micro	0.15	0.11	0.11	0.15	0.121
Micro&Nano	0.17	0.17	0.18	0.22	0.201

When the gap ratios were calculated for three different liquids (Table 6), it was observed that the differences in liquid energies affected the wetting significantly, and the determinativeness of nanoroughness was observed. The highest wettability was presented in the diiodomethane with the lowest surface energy and the lowest wettability in the water with the highest free surface energy. Due to the increase of nanoroughness in the series from 1M to 4M, the gap ratio increased in 3 liquids, but the gap ratio in the 5M sample decreased. As can be observed from the roughness measurements, in case of 5M sample when the abrasive grain size decreases due to the abrasive mesh size, it cannot reveal a new surface and even erodes the existing micro-size roughness.

4. Discussion

As a result, an evaluation can be made by accepting the presence of structures of hydrophobic characters, such as airbags/cavities, in chemically pure samples with unexpected apparent contact angle values. In this respect, the proposed air package structure; is presented as component "b" of the Cassie - Baxter approach, which is the most advanced equation considering roughness. Finally, five samples under three different liquids were found to produce unlike f_{LV} values (gap ratio). When the Cassie-Baxter approach and micro-nano roughness values are evaluated together, it is possible to test a structure defined as hierarchical roughness in the literature (Bormashenko & Starov, 2013; Gogolides et al., 2015). Whether or not a liquid bridges a solid topographic recess on this stage, or whether it will raid a valley is not only dependent on the geometry of the substrate. Furthermore, it depends on whether the solid wetting energy of that liquid can overcome the sum of the internal pressure of the underlying air, the viscosity of the liquid, the film resistance, and the liquid disjoining pressure (Chau et al., 2009; Nosonovsky & Bhushan, 2009).

Wu et al. (2016), mentioned the existence of hierarchical structured natural surfaces in his study, he stated that hierarchical structures might have different transition theories. His research includes computational applications, and the artificial surfaces differ from the actual surfaces in nature by having well-defined geometric constants. As in the present example, it was found that the surface had a transition zone with CB, W - W, W and CB, CB-W, W, with randomly distributed roughness S_a and

the corresponding S_{dr} values. Depending on the liquid surface energy the transitions range from lowest air ratio of 17% with diiodomethane on 1M sample represent transition "CB-W→W-W transition" of Fig. 8, to highest air ratio of 34.6% with pure water on 4M sample may represent a transition "CB-CB→W-W transition" of Fig. 9.

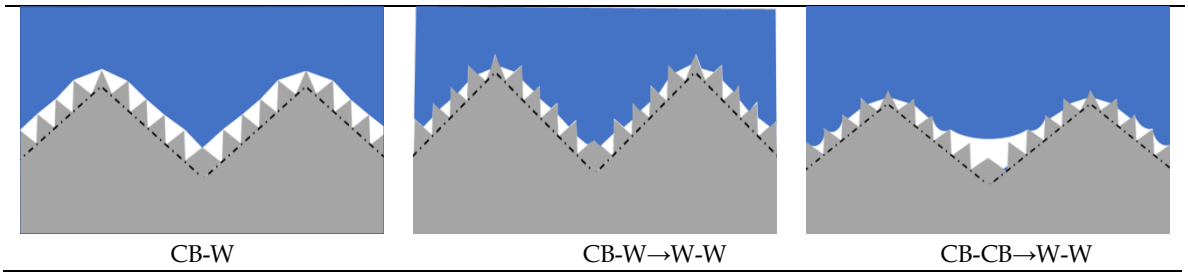

Fig. 9. Transition alternatives proposed for the hierarchical structure

5. Conclusion

At this stage, it was seen that the solid surface energy could not be determined and the resulting inconsistency could be regulated only by modifying the Cassie - Baxter approach. Furthermore, the existence of air packs under the water droplet not foreseen by previous studies was calculated, and it was determined that there could be at least 26% and 35% air package on these surfaces under water.

As a result of the investigation, it has been determined that micro and nano surface roughness can be changed on a marble surface, and nano air packages can be formed on the natural stones after using a common industrial natural stone surface treatment process.

Acknowledgement

Authors sincerely thanks to Prof. Mehmet Sabri Çelik and his Lab Crew for providing the opportunity to work in Istanbul Technical University, Mineral Processing Department, further thanks to Afyon Kocatepe University, Mining Engineering Department for their kind support.

References

AHMED, M. M. (2010). *Effect of comminution on particle shape and surface roughness and their relation to flotation process*. International Journal of Mineral Processing, 94(3–4), 180–191. https://doi.org/10.1016/j.minpro.2010.02.007

BORMASHENKO, E., STAROV, V. (2013). *Impact of surface forces on wetting of hierarchical surfaces and contact angle hysteresis*. Colloid and Polymer Science, *291*(2), 343–346. https://doi.org/10.1007/s00396-012-2785-9

CASSIE, B. D., CASSIE, A. B. D., BAXTER, S. (1944). *Wettability of Porous Surfaces*. Transactions of the Faraday Society, 40(5), 546–551. https://doi.org/10.1039/tf9444000546

CHAU, T. T., BRUCKARD, W. J., KOH, P. T. L., NGUYEN, A. V. (2009). *A review of factors that affect contact angle and implications for flotation practice*. Advances in Colloid and Interface Science, 150(2), 106–115. https://doi.org/10.1016/j.cis.2009.07.003

CHOI, W., TUTEJA, A., MABRY, J. M., COHEN, R. E., MCKINLEY, G. H. (2009). *A modified Cassie-Baxter relationship to explain contact angle hysteresis and anisotropy on non-wetting textured surfaces*. Journal of Colloid and Interface Science, 339(1), 208–216. https://doi.org/10.1016/j.jcis.2009.07.027

DITSCHERLEIN, L., FRITZSCHE, J., PEUKER, U. A. (2016). *Study of nanobubbles on hydrophilic and hydrophobic alumina surfaces*. Colloids and Surfaces A: Physicochemical and Engineering Aspects, 497(March), 242–250. https://doi.org/10.1016/j.colsurfa.2016.03.011

DORRER, C., RÜHE, J. (2009). *Some thoughts on superhydrophobic wetting*. Soft Matter, 5(1), 51. https://doi.org/10.1039/b811945g

FOWKES, F. M. (1963). *Additivity of Intermolecular Forces at Interfaces. I. Determination of The Contribution to Surface and Interfacial Tensions of Dispersion Forces in Various Liquids 1*. The Journal of Physical Chemistry, 67(12), 2538–2541. https://doi.org/10.1021/j100806a008

FRITZSCHE, J., PEUKER, U. A. (2014). *Particle adhesion on highly rough hydrophobic surfaces: The distribution of*

interaction mechanisms. Colloids and Surfaces A: Physicochemical and Engineering Aspects, 459, 166–171. https://doi.org/10.1016/j.colsurfa.2014.07.002

GAO, N., & YAN, Y. (2009). *Modeling Superhydrophobic Contact Angles and Wetting Transition*. Journal of Bionic Engineering, *6*(4), 335–340. https://doi.org/10.1016/S1672-6529(08)60135-3

GOGOLIDES, E., ELLINAS, K., TSEREPI, A. (2015). *Hierarchical micro and nano structured, hydrophilic, superhydrophobic and superoleophobic surfaces incorporated in microfluidics, microarrays, and lab on chip microsystems*. Microelectronic Engineering, 132, 135–155. https://doi.org/10.1016/j.mee.2014.10.002

GREßLER, S., FIEDELER, U., SIMKÓ, M. (2010). *Self-cleaning , dirt and water-repellent coatings on the basis of nanotechnology*. Nano Trust Dossiers, 1–6.

GÜRCAN, S., ÖZTÜRK, E. (2014). *The Effects of Different Abrasives on Some Limestone Polishing Process*. Afyon Kocatepe University Journal of Sciences and Engineering, 14(2), 1–11. https://doi.org/10.5578/fmbd.7494

HAMPTON, M. A., & NGUYEN, A. V. (2010). N*anobubbles and the nanobubble bridging capillary force. A*dvances in Colloid and Interface Science, 154(1–2), 30–55. https://doi.org/10.1016/j.cis.2010.01.006

HE, Y., JIANG, C., CAO, X., CHEN, J., TIAN, W., YUAN, W. (2014). *Reducing ice adhesion by hierarchical micro-nano-pillars*. *Applied Surface Science*, 305, 589–595. https://doi.org/10.1016/j.apsusc.2014.03.139

HEJAZI, V. (2014). *Wetting, Superhydrophobicity, and Icephobicity* in Biomimetic Composite Materials, (May), 185.

HEJAZI, V., MOGHADAM, A. D., ROHATGI, P., NOSONOVSKY, M. (2014). *Beyond Wenzel and Cassie − Baxter : Second-Order Effects on the Wetting of Rough Surfaces*, (c).

HICYILMAZ, C., ULUSOY, U., BILGEN, S., YEKELER, M. (2005). *Flotation responses to the morphological properties of particles measured with three-dimensional approach.* International Journal of Mineral Processing, 75(3–4), 229–236. https://doi.org/10.1016/j.minpro.2004.08.019

ITHERM, S. (2015). *Dynamic wetting on superhydrophobic surfaces : Droplet impact and wetting hysteresis The MIT Faculty has made this article openly available.* Dynamic Wetting on Superhydrophobic Proceedings of the 12th IEE.

JUNG, Y. C., BHUSHAN, B. (2008). *Wetting behaviour during evaporation and condensation of water microdroplets on superhydrophobic patterned surfaces*. Journal of Microscopy, 229(1), 127–140. https://doi.org/10.1111/j.1365-2818.2007.01875.x

KARAKAS, F., HASSAS, B. V. (2016). *Effect of surface roughness on interaction of particles in flotation.* Physicochemical Problems of Mineral Processing, 52(1), 18-34..

KIM, P., KREDER, M. J., ALVARENGA, J., AIZENBERG, J. (2013). *Hierarchical or not? Effect of the length scale and hierarchy of the surface roughness on omniphobicity of lubricant-infused substrates.* Nano Letters, 13(4), 1793–1799. https://doi.org/10.1021/nl4003969

LAMARCHE, C. Q., LEADLEY, S., LIU, P., KELLOGG, K. M., HRENYA, C. M. (2017). *Method of quantifying surface roughness for accurate adhesive force predictions.* Chemical Engineering Science, 158, 140–153. https://doi.org/10.1016/j.ces.2016.09.024

LIU, K., YAO, X., JIANG, L. (2010). *Recent developments in bio-inspired special wettability.* Chemical Society Reviews, 39(8), 3240–3255. https://doi.org/10.1039/b917112f

MA, M., HILL, R. M., BICO, J. (2006). *Superhydrophobic surfaces*. Current Opinion in Colloid & Interface Science, *11*(4), 193–202. https://doi.org/10.1016/j.cocis.2006.06.002

MATZIARIS, K., PANAYIOTOU, C. (2014). *Tunable wettability on Pendelic marble: Could an inorganic marble surface behave as a "self-cleaning" biological surface*? Journal of Materials Science, 49(5), 1931–1946. https://doi.org/10.1007/s10853-013-7902-8

MILNE, A. J. B., AMIRFAZLI, A. (2012). T*he Cassie equation: How it is meant to be used*. Advances in Colloid and Interface Science, 170(1–2), 48–55. https://doi.org/10.1016/j.cis.2011.12.001

MURAKAMI, D., JINNAI, H., & TAKAHARA, A. (2014). *Wetting transition from the cassie-baxter state to the wenzel state on textured polymer surfaces.* Langmuir, 30(8), 2061–2067. https://doi.org/10.1021/la4049067

NEUMANN, A. W., GOOD, R. J., HOPE, C. J., & SEJPAL, M. (1974). *An equation-of-state approach to determine surface tensions of low-energy solids from contact angles.* Journal of Colloid And Interface Science, 49(2), 291–304. https://doi.org/10.1016/0021-9797(74)90365-8

NOSONOVSKY, M., & BHUSHAN, B. (2009). *Multiscale effects and capillary interactions in functional biomimetic surfaces for energy conversion and green engineering.* Philosophical Transactions. Series A, Mathematical, Physical, and Engineering Sciences, 367, 1511–1539. https://doi.org/10.1098/rsta.2009.0008

OWENS, D. K., & WENDT, R. (1969). *Estimation of the Surface Free Energy of Polymers.* Journal of Applied Polymer

Science, 13, 1741–1747. https://doi.org/10.1592/phco.30.10.1004

RAHIMI, M., DEHGHANI, F., REZAI, B., ASLANI, M. R. (2012). I*nfluence of the roughness and shape of quartz particles on their flotation kinetics.* International Journal of Minerals, Metallurgy, and Materials, 19(4), 284–289. https://doi.org/10.1007/s12613-012-0552-z

STAROV, V. M. (2010). *Nanoscience : colloidal and interfacial aspects.*

SU, C. (2010). *Facile fabrication of a lotus-effect composite coating via wrapping silica with polyurethane.* Applied Surface Science, 256(7), 2122–2127. https://doi.org/10.1016/j.apsusc.2009.09.058

TANTUSSI, G., & LANZETTA, M. (2007). *Analyses of stone surfaces by optical methods.* In AI Te. M 2007, 8th Conference of the Italian Association of Mechanical Technology (pp. 100–128).

VAN OSS, C. J., CHAUDHURY, M. K., & GOOD, R. J. (1988). *Interfacial Lifshitz-van der Waals and polar interactions in macroscopic systems.* Chemical Reviews, 88(6), 927–941. https://doi.org/10.1021/cr00088a006

VAZIRI HASSAS, B., CALISKAN, H., GUVEN, O., KARAKAS, F., CINAR, M., & CELIK, M. S. (2016). *Effect of roughness and shape factor on flotation characteristics of glass beads.* Colloids and Surfaces A: Physicochemical and Engineering Aspects, 492, 88–99. https://doi.org/10.1016/j.colsurfa.2015.12.025

WANG, L., WANG, X., WANG, L., HU, J., WANG, C. L., ZHAO, B., ZHANG, L. (2017). F*ormation of surface nanobubbles on nanostructured substrates.* Nanoscale, 9(3), 1078–1086. https://doi.org/10.1039/c6nr06844h

WANG, X., ZHAO, B., MA, W., WANG, Y., GAO, X., TAI, R., ZHANG, L. (2015). *Interfacial nanobubbles on atomically flat substrates with different hydrophobicities.* Chem. Phy.s. Chem, *16*(5), 1003–1007. https://doi.org/10.1002/cphc.201402854

WEBB, H. K., CRAWFORD, R. J., IVANOVA, E. P. (2014). *Wettability of natural superhydrophobic surfaces.* Advances in Colloid and Interface Science, 210(22), 58–64. https://doi.org/10.1016/j.cis.2014.01.020

WENZEL, R. N. (1936). *Resistance of solid surfaces to wetting by water.* Industrial and Engineering Chemistry, 28(8), 988–994. https://doi.org/10.1021/ie50320a024

WU, H., ZHU, K., WU, B., LOU, J., ZHANG, Z., CHAI, G. (2016). *Influence of structured sidewalls on the wetting states and superhydrophobic stability of surfaces with dual-scale roughness.* Applied Surface Science, 382, 111–120. https://doi.org/10.1016/j.apsusc.2016.04.101

WU, W., GIESE, R. F., VANOSS, C. J. (1996). *Change in surface properties of solids caused by grinding.* Powder Technology, 89(2), 129–132. https://doi.org/10.1016/S0032-5910(96)03158-0

YEKELER, M., ULUSOY, U., & HIÇYILMAZ, C. (2004). *Effect of particle shape and roughness of talc mineral ground by different mills on the wettability and floatability.* Powder Technology, 140(1–2), 68–78. https://doi.org/10.1016/j.powtec.2003.12.012

YOUNG, T. (1805). *An Essay on the Cohesion of Fluids.* Philosophical Transactions of the Royal Society of London, 95(0), 65–87. https://doi.org/10.1098/rstl.1805.0005

ZHAO, J.-J., DUAN, Y.-Y., WANG, X.-D., WANG, B.-X. (2013). *Effect of Nanostructured Roughness on Evaporating Thin Films in Microchannels for Wenzel and Cassie–Baxter States.* Journal of Heat Transfer, 135(4), 041502. https://doi.org/10.1115/1.4023230

ZISMAN, W. A. (1964). *Relation of the Equilibrium Contact Angle to Liquid and Solid Constitution.* Contact Angle, Wettability, and Adhesion, 43(43), 1–51. https://doi.org/doi:10.1021/ba-1964-0043.ch001\n10.1021/ba-1964-0043.ch001